

Supernova remnants and the origin of the cosmic radiation: the electron component

This article has been downloaded from IOPscience. Please scroll down to see the full text article.

2002 J. Phys. G: Nucl. Part. Phys. 28 359

(<http://iopscience.iop.org/0954-3899/28/3/301>)

[The Table of Contents](#) and [more related content](#) is available

Download details:

IP Address: 128.122.52.218

The article was downloaded on 22/07/2009 at 19:15

Please note that [terms and conditions apply](#).

Supernova remnants and the origin of the cosmic radiation: the electron component

A D Erlykin^{1,2} and A W Wolfendale¹

¹ Department of Physics, University of Durham, South Road, Durham, DH1 3LE, UK

² P N Lebedev Physics Institute, Leninsky Prospekt, Moscow, Russia

Received 17 October 2001, in final form 14 December 2001

Published 1 February 2002

Online at stacks.iop.org/JPhysG/28/359

Abstract

The model adopted by us in previous work (Erlykin A D and Wolfendale A W 2001a, 2001b, 2001c involving the production of cosmic rays by supernova remnant (SNR) shocks has been used to make predictions for the electron component. It is found that the well-known low e/p ratio ($\sim 1\%$ at 10 GeV), and a somewhat steeper electron spectrum, even in the energy region where energy losses due to synchrotron and inverse Compton processes are small, follows if it is assumed that the injection efficiency falls with increasing Mach number of the shock.

It must be stated, however, that the Mach number argument is not firmly based; nevertheless if it is not a Mach number effect, it is something that simulates it.

Irrespective of the validity of the injection efficiency arguments, the Monte Carlo calculations of cosmic ray propagation from randomly distributed SNR have validity, it is found that electron energies just above the maximum of those detected experimentally are needed in order to check on the predictions of our 'single source model', which we claim has particular relevance in the case of the more massive cosmic rays.

A brief discussion of the relevance of our arguments to electrons in other galactic and extragalactic environments is given.

1. Introduction

Although electrons form only $\sim 1\%$ of the cosmic ray intensity (at 1–10 GeV) as measured at the Earth, their importance for astronomy in general is very great; this importance follows from the fact that much of our knowledge about the Universe comes from radiation produced by the movement of electrons. All wavelengths are involved, from radio waves to gamma rays.

Radioastronomy is an obvious example, where most of the radio waves are generated by electrons spiralling in cosmic magnetic fields. The synchrotron radiation from galactic cosmic

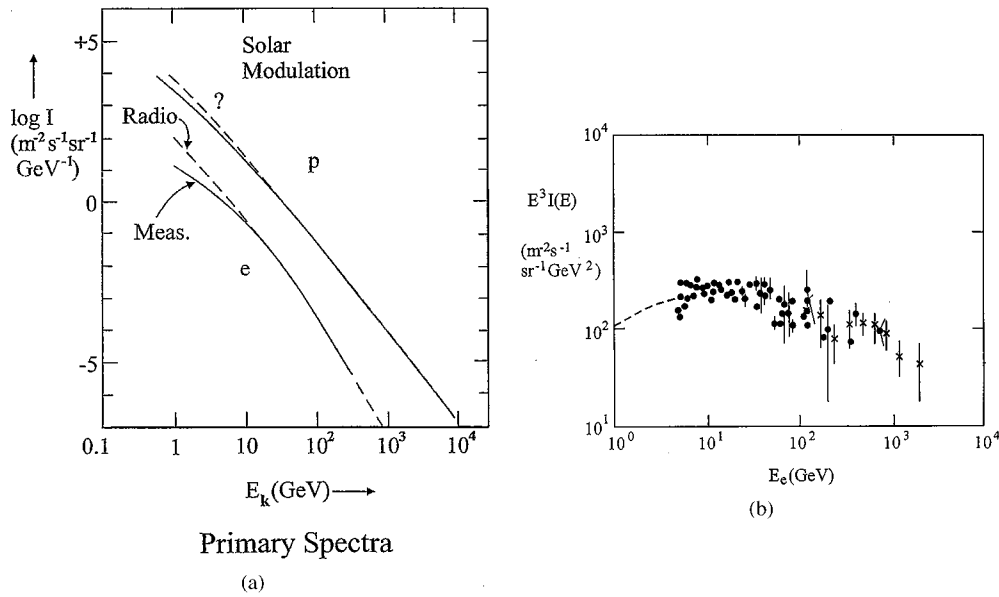


Figure 1. (a) Comparison between the measured electron and proton energy spectra. Although absolute intensities are given it will be appreciated that there are systematic errors present in the various datasets and these are reflected in the values shown. The systematic errors are typically $\pm 35\%$. Nevertheless, the spectral shapes are reasonably accurate. The question mark for the p -spectrum indicates the likely spectrum after correction for solar modulation. The electron spectrum marked 'radio' is that derived from studies of radio synchrotron radiation and corrected for free-free absorption in the ISM (after Strong and Wolfendale 1978, Webber *et al* 1992). (b) Compendium of results on the measured electron spectrum at the Earth and our 'best line'. The sources of the data are: Kobayashi *et al* (1999), Golden *et al* (1984), Torii *et al* (1997), Tang (1984), Barbiellini *et al* (1997), HEAT (Barwick *et al* 1998), Golden *et al* (1994) and CAPRICE 2000 (Boezio *et al* 2000). The crosses relate to the extensive study of Kobayashi *et al*. Above 100 GeV, the precise data are from HEAT and CAPRICE. The errors indicated are statistical only. Below 10 GeV there are serious problems with solar modulation; the dashed line represents our estimate from figure 1 (radio). A 'best line' is shown in figure 4(a).

ray electrons is a case in point, and in this case, unlike the situation for 'discrete' radio sources (such as pulsars), the electrons are to be identified with 'local' cosmic ray electrons and the magnetic field is the general, somewhat tangled, galactic magnetic field of strength of some few microGauss. As an example, at 408 MHz, where detailed intensity maps are available (e.g. Haslam *et al* 1981), the cosmic ray electron energies are mainly in the range 10–20 GeV.

Figure 1(a) shows the general situation for the measured electron and proton energy spectra; also shown is an extrapolation to lower energies for electrons by way of radio data (Strong and Wolfendale 1978, Webber *et al* 1992). Figure 1(b) is a compendium of measurements for electrons. It is confidently asserted that the steepening of the electron spectrum beyond about 100 GeV is due to energy losses, largely by way of synchrotron and inverse Compton processes in the interstellar medium (ISM).

Although it is often stated that supernova remnants (SNR) are probably responsible for the cosmic ray electrons, there appears to have been no detailed calculations in which the evolution of the electron energy spectrum is examined from the very beginning of particle acceleration and the stochastic nature of SN explosions in the galaxy is taken into account. Even when the fluctuations in the spacetime distribution were considered (Pohl and Esposito 1998), the injection spectrum was taken as an input parameter, which was then fitted to the

experimental data. In most of the other papers (e.g. Syrovatskii 1959, Shen 1970, Shen and Mao 1971, Stephens 1990, Aharonian *et al* 1995, Atoyan *et al* 1995, Nishimura *et al* 1995, Moskalenko and Strong 1998, Kobayashi *et al* 1999) the electron spectrum was calculated solving the transport equation with a continuous injection term, modified in some cases by the accidental presence of discrete nearby and recent sources, or by some known sources each with a fixed age and distance from the solar system.

Before continuing, it is necessary to mention the minority positron component. Of considerable importance in its own right—insofar as it relates mainly, and probably entirely, to the secondary component produced by protons and heavier nuclei interacting with the ISM nuclei—it is numerically small, in comparison with the electron component. Specifically, $e^+/(e^+ + e^-)$ is always less than 20% at energies above about 2 GeV, and is disregarded here, namely, by ‘electrons’ we mean primarily the electrons produced by acceleration processes in the galaxy. However, a brief mention of one specific aspect of positrons is made later (see section 5.2).

In the present paper we deal with the following problems:

- (i) the injection problem; specifically, why the e/p ratio is so low,
- (ii) the spectrum emerging from the SNR when it allows free exit of the accelerated particles,
- (iii) the predicted spectra and their exponents,
- (iv) the contribution to the high-energy intensity from a ‘single source’, and
- (v) the frequency distribution of predicted curvature in the energy spectrum.

Also included are a brief study of the contribution from specific local SN and the implications for the proton spectrum of the evolution of the Alfvén wave spectrum and consequent (slight) dependence of injection efficiency on time.

2. The calculations

2.1. The model

In our model (EW 2001a, 2001b) particles (protons and heavier nuclei) are accelerated throughout the lifetime of the remnant. The computer code for electrons is essentially the same as for protons and other nuclei but with three modifications:

- (i) the kinematic effect connected with the use of the electron rest mass, m_e ,
- (ii) inefficiency of electron acceleration by strong shocks with high Mach numbers (by which is meant that the yield is smaller than predicted by the simple SNR acceleration model—but the spectral shape is unchanged),
- (iii) energy losses: compared with protons of the same energy, electrons have higher energy losses due to bremsstrahlung, synchrotron radiation and inverse Compton scattering during both the expansion and diffusion phases.

The energy losses have been included in the manner appropriate to the conditions in the ISM by

$$-\frac{dE}{dt} = \beta(E) = a + bE + cE^2. \quad (1)$$

If the energy E is in GeV and the energy losses $\beta(E)$ are in GeV s^{-1} , then the coefficients a, b, c have the following values (Atoyan *et al* 1995): $a = 3.07 \times 10^{-16}n$, $b = 1.0 \times 10^{-15}n$, $c = 1.01 \times 10^{-16}w$, where n is the matter density in atom cm^{-3} and w is the energy density in eV cm^{-3} , contained in the optical, infrared and microwave radiation and also in the magnetic field. The calculations are divided into two parts, for the galactic disk and the galactic halo,

each with its appropriate loss parameters. It is necessary at this stage to explain what is meant by ‘disk’ and ‘halo’. For ease of calculation we define the former as that part of the galaxy for which we can take the diffusion coefficient as being constant (with respect to height above the plane, z) and equal to the local value. The value of the scale height for the disk is taken as 1 kpc (as in EW 2001a), this value being the half-height of the square of the magnetic field (French 1977). The halo is a much more extended region, the height of which is subject to considerable doubt; for example, some consider that there is significant galactic plasma as far as the Magellanic clouds (50–60 kpc away) but, in a sense, its height is not too important in our case: the halo represents a reservoir from which particles which have escaped from the disk can re-enter it.

The disk is more important in the sense that the solar system is within the disk, as are the likely sources (SNR in this case). The effect of particles which escape into the halo and re-enter later is considered in an approximate fashion and the halo contribution is added at the end. Such re-entrant particles were considered in an earlier paper as a possible way of explaining the fact that the radial gradient of the cosmic ray intensity is so much smaller than that of the likely sources (Erlykin *et al* 1996).

The parameters of the disk are determined, allowing for the z -dependence of the ISM gas density, optical radiation and magnetic field, and for the energy loss parameters we adopt $n = 0.2 \text{ cm}^{-3}$, $w_{\text{opt}} = 0.4 \text{ eV cm}^{-3}$ and $w_B = 0.3 \text{ eV cm}^{-3}$. The energy density of the microwave background radiation has been taken as $w_{\text{mwb}} = 0.25 \text{ eV cm}^{-3}$.

Following the situation for protons we assume that the diffusion of electrons starts only after the expansion phase is finished. As for the energy losses of the electrons, however, these start immediately after their creation, i.e. even during the expansion phase. Therefore, the ‘instant’ energy spectrum of electrons $\frac{dI}{dE_0}(E_0, t)$ created at the moment t during the expansion changes at the end of expansion T_e as

$$\frac{dI}{dE}(E, T_e, t) = \frac{dI}{dE_0}(E_0, t) \frac{dE_0}{dE}(E, T_e - t) \quad (2)$$

where E_0 and E are connected by

$$\int_E^{E_0} \frac{dE'}{\beta(E')} = T_e - t. \quad (3)$$

The final spectrum at the end of the expansion phase is the integral of all the instant spectra over t :

$$I_0(E, T_e) = \int_0^{T_e} \frac{dI}{dE dt'}(E, T_e, t') dt'. \quad (4)$$

After the expansion phase the electrons diffuse in the usual manner and lose energy during their propagation. The diffusion ‘radius’ R_d is determined, as in Syrovatskii (1959), by

$$R_d(E) = 2\sqrt{\int_E^{E_0} \frac{D(E')}{\beta(E')} dE'}. \quad (5)$$

The intensity of electrons decreases in a manner similar to that of protons (EW 2001a), the only difference being that the exponential escape term, $\exp(-\frac{t-T_e}{\tau})$, is replaced by $\exp(-\int_E^{E_0} \frac{dE'}{\beta\tau})$, where E_0 is determined by

$$\int_E^{E_0} \frac{dE'}{\beta(E')} = t - T_e \quad (6)$$

and τ is the escape time.

For the galactic halo contribution we take the energy spectrum calculated for be appropriate for the escaping particles and adopt a scale height higher than H_G by a factor of 10 and a lifetime against escape similarly higher by 10. The result is that the diffusion coefficient is also higher than that for the disk by a factor of 10—a result in accordance (approximately) with the lower magnetic field in this region.

2.2. The injection efficiency for electrons

2.2.1. The problems for the electron component. The most dramatic problem for cosmic ray electrons is an explanation of the fact that the e/p ratio is so low, typically $\sim 1\%$ at 10 GeV, when the densities of free electrons and protons in the ISM are virtually the same. Also important, but not as dramatic, is the fact that the measured energy spectra of electrons and protons have somewhat different exponents in the energy region ($\lesssim 100$ GeV) where energy losses are not expected to be serious and cannot be invoked to explain the steepness.

In what follows we consider various attempts which have been made to explain the problems just referred to, starting with the small e/p ratio.

2.2.2. The small e/p ratio: an empirical approach. We start with the empirical approach adopted by Berezhko *et al* (1996) in order to explain the excessive intensities of nuclei heavier than protons in comparison with the expectation from the known abundances of these nuclei in the ISM. Berezhko *et al* start by defining an ‘injection efficiency’ for protons which is typically in the range 10^{-3} – 10^{-4} , the value being dependent on the conditions in the ISM (density and temperature) and chosen to give the experimentally measured spectrum after the acceleration mechanism has been applied. They then go on to argue that η will be a simple function of A/Z' for nuclei, where Z' is the actual charge on the nucleus when in the pre-acceleration region, i.e. in the general ISM. If acceleration is in the ‘warm ISM’, of modest temperature (typically $\sim 10^4$ K), then $Z' = 1$ and thus $\eta = f(A)$, Berezhko *et al* write $\eta \propto A^\beta$ and quote $\beta = 0.8$ as being needed to fit the data.

Continuing with this empirical approach we can make an order of magnitude estimate of e/p by assuming that the A^β has validity down to the electron mass (it could be argued that this is ‘unphysical’ but insofar as the whole ‘ β -approach’ is empirical it is no worse for electrons than for ions). The result follows simply as $e/p = 1837^{-0.8} = 0.25\%$. Interestingly, this value is only about a factor of four different from what is needed.

We are mindful of the fact that there are other possibilities for injection, including the model of Ellison *et al* (1997), involving grains in the ISM. Insofar as we consider that SN exploding in the HISM, which has been previously seeded by other SN, is the basis of our model (Erlykin *et al* 1998), then the conditions for grain production may not be appropriate, at least for all CR, although it must be said that at low energies the precise composition data seem to favour the grain model (in which the bulk of the accelerated particles are a ‘well mixed’ ISM). A model involving the HISM (specifically the local bubble) has also been put forward by Higdon *et al* (1999).

2.2.3. The small e/p ratio: the underlying physics. A common argument to explain the low e/p ratio may well be the physics behind the empirical relation. Specifically, for electrons, Ellison and Reynolds (1991) argue that thermal electrons have gyroradii 43 (i.e. $\sqrt{m_p/m_e}$) times smaller than for thermal protons of the same kinetic energy so that if the waves in the shock—generated in part by the cosmic rays themselves—have too few short wavelengths to scatter the electrons then they, the electrons, will be accelerated very infrequently. That the density of waves increases with wavelength is in accordance with the fact that high A (with charge $Z' = 1$) will have longer wavelength where waves are more common than those for

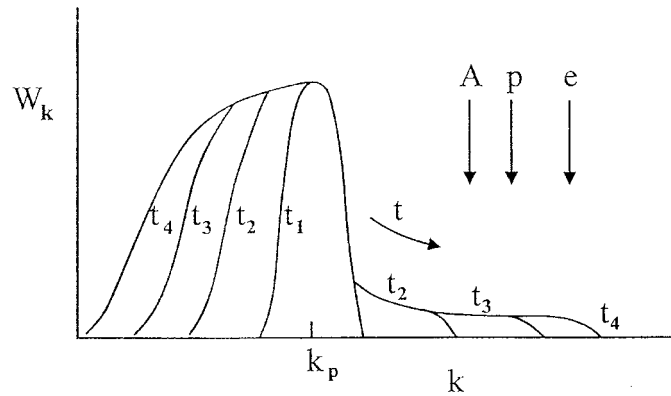


Figure 2. Schematic diagram of the distribution of Alfvén waves of wave number k ($k = \frac{2\pi}{L}$), from the analysis of Kaplan and Tsytovich (1973) (which actually refers to Langmuir turbulence but the situation is similar). The energy is injected as a step function at $k = k_p$ and as time progresses it moves down to both smaller and larger k -values, the latter corresponding to smaller distance scales. The positions of thermal e , p and nuclei A (of the same kinetic energy) are indicated in a very approximate fashion. It is assumed that $T_e = T_p = T_A$ in this plot.

protons of the same energy. This then, could well be the reason for the $A^{0.8}$ dependence of Berezhko *et al* (and the $A^{0.6}$ dependence of EW 2001c). Figure 2 gives a schematic description of the situation (after Kaplan and Tsytovich 1973).

2.2.4. A non-constant injection efficiency. The need for the spectrum of electrons produced by an SNR to be steeper than the standard E^{-2} spectrum expected for shock acceleration is well known; for example, Kobayashi *et al* (1999) adopt $\gamma = 2.4$. It is true that our preferred acceleration model, following Axford (1981), gives an ‘input spectrum’ somewhat steeper than E^{-2} , namely, $E^{-2.15}$, but this is still too flat. The same problem arises for protons, to some extent, and this aspect will be considered later.

No doubt there are a number of ways in which a steeper input spectrum can be achieved. Using the various radio spectral shapes determined for different SNR, Busching *et al* (2001) assume that there is a Gaussian spread in the indices for particle production, protons in their case. A similar situation could be assumed for electrons, ‘favourable’ fluctuations could then be invoked to explain the local, steep electron spectrum. We prefer, however, to go back to the SNR acceleration mechanism and perturb it in what might be a physically reasonable fashion so as to give the steeper injection spectrum. The particles produced in this way are then trapped in the SNR, where the highest energy particles suffer energy losses before giving the ‘emergent spectrum’ at an SNR radial distance of ~ 100 pc.

We postulate that the injection efficiency depends on the Mach number and this possibility is considered in section 2.2.5. A possible reason for such a dependence relates to the temperature of electrons and protons which may be different and such differences may persist in the shocked mode of the gas prior to acceleration to relativistic energies. Indeed, the whole question of injection efficiency for electrons and its dependence on temperature and other parameters is a matter of great complexity (e.g. Shimada and Hoshino 2000) involving, as it does, the development of large instabilities.

There is evidence for such temperature differences in dense molecular clouds (e.g. D R Flower Private communication)—although this is hardly relevant here—however, such differences occur even in low density environments closer to the densities considered here. Thus, Pineau des Forêts *et al* (1987) find that for shocks of velocity 15 km s^{-1} in gas of 5 cm^{-3}

(HI) and 10 cm^{-3} (H_2) and a field of $5 \mu\text{G}$, the maximum temperatures are $T_p \sim 7 \times 10^3 \text{ K}$ and $T_e \sim 5 \times 10^3 \text{ K}$. It is reassuring, and to be expected, that T_e approaches T_p as the Mach number falls.

Such gas densities are, admittedly, high compared with the HISM, which has density $\sim 3 \times 10^{-3} \text{ cm}^{-3}$ (e.g. Berezhko *et al* 1996); however, they are not far from the density in the warm interstellar medium (WISM): $\simeq 0.3 \text{ cm}^{-3}$ and it is not unlikely that the WISM plays an important role in the acceleration of the ‘low’ energy electrons, unlike the HISM, which is thought to be a prerequisite for high energy protons.

2.2.5. An injection efficiency depending on Mach number. As remarked already, notwithstanding some general arguments regarding pre-shocked electron temperatures, the M -dependent efficiency argument is essentially *ad hoc*. However, attention must be drawn to a very recent study by Schmitz *et al* (2001) which shows that the efficiency for electron injection rises as the ratio of kinetic pressure/magnetic pressure falls, although it must be said that for the case where all other parameters are the same the efficiency *increases* with M . We expect this ratio to fall as M falls and, if so, $\eta(M)$ will fall with increasing M .

We have made estimates for a form of $\eta(M)$: $\eta = \exp - (M/M_0)^2$, M_0 being a constant, and this is our preferred choice. Calculations have been made for this form and also for $\exp - (M/M_0)$. Unfortunately, so far, at least, there is no theoretical guidance on what value M_0 should take nor which expression is more appropriate; here we take the former. Figure 3(a) shows the results of three trials for the first expression. It is interesting to note that the main effect of decreasing M_0 is to reduce the intensity, the increase in exponent is slight.

In terms of reproducing the ‘correct’ e/p ratio, $M_0 = 2$ appears to be best, as will be seen later, and in what follows it will be adopted.

A final mark about our assumption of an M -dependent efficiency is that this is just one way of generating the required steeper electron spectrum; presumably there are others, too, but we do not know of them.

2.3. The emergent spectrum of electrons

2.3.1. Sensitivity to the parameters. The spectrum of electrons (as distinct from protons) emerging from the SNR will depend on a number of parameters, mainly the different rest masses, smaller acceleration efficiency of strong shocks and additional energy losses for electrons. Figure 3(b) illustrates the formation of the electron emergent spectrum for the standard radius of expansion, $R_e = 100 \text{ pc}$, and shows the contributions to the emergent spectrum from different time zones. The gradual steepening of the spectrum is apparent, as is the drawing in of the maximum energy at short times because of energy loss in the long transit time to escape. It is appropriate to remark that the relatively sharp cut-off in intensity at the maximum energy is a consequence of the pile-up that occurs as higher input energies give an asymptotic emergent energy. No fluctuations in energy loss are included in this simple treatment. In fact, they *will* occur in the remnant because of variations in the energy densities of magnetic fields and starlight along the paths followed and in the ISM, in general, for the same reason. An estimate of their likely effect is given later. The emergent spectrum of electrons is steeper ($\gamma_e = 2.49$) than that for protons ($\gamma_p = 2.15$), as a consequence of the adopted assumption of the inefficiency of strong shocks for the acceleration of electrons which was, of course, designed to give this result.

A key quantity for electrons (but not as important for protons) is the SNR radius, R_e , at which the particles are allowed to ‘escape’ from the confines of the SNR and diffuse thereafter. In EW (2001a), and here, we adopt $R_e = 100 \text{ pc}$ as the best estimate. A number of factors

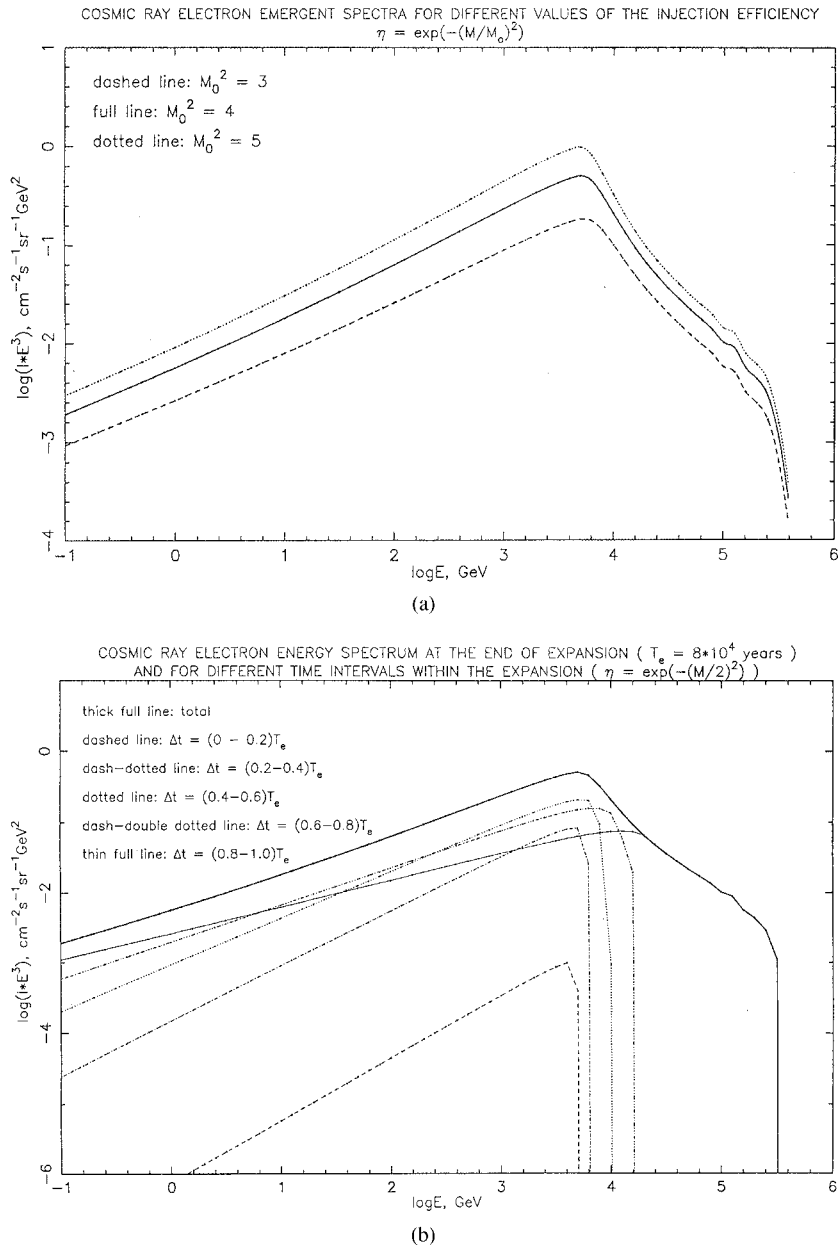


Figure 3. (a) Spectra of electrons emerging from an SNR for different values of the efficiency factor, M_0 , in the expression $\nu(M) = \exp(-(M/M_0)^2)$. (b) Spectra of electrons emerging from an SNR accelerated in different time intervals. It will be noted that later spectra are steeper, a result understandable in terms of the smaller Mach numbers at later times. It is assumed here that the injection efficiency, η , is dependent on the Mach number in the manner shown. (c) Emergent spectra for alternative values of R_e , the radius of the remnant at the end of the expansion phase. The values of R_e , 75 and 125 pc, represent the likely limits in practice. (d) Emergent spectra for variants of the energy loss parameter, c , which allow for different paths—and thereby different energy losses—in the SNR and in the ISM in general.

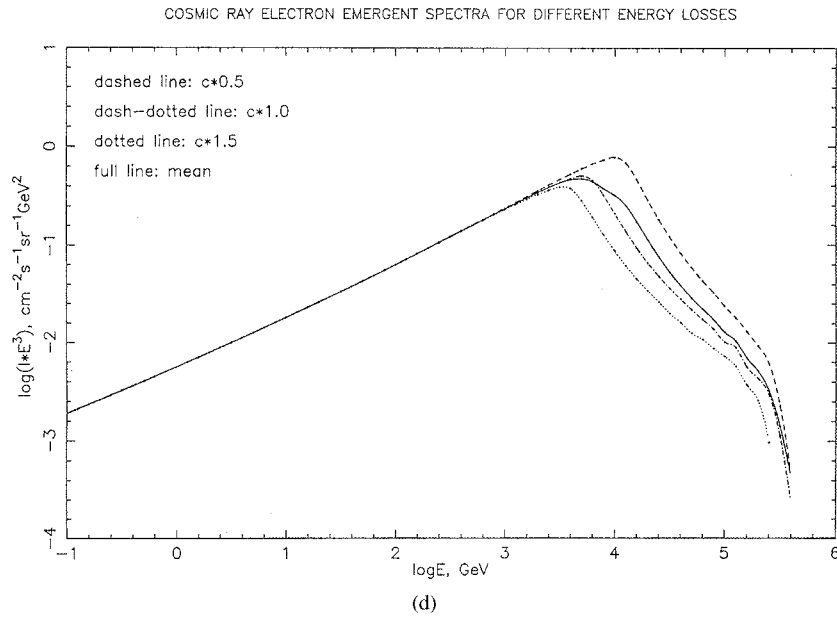
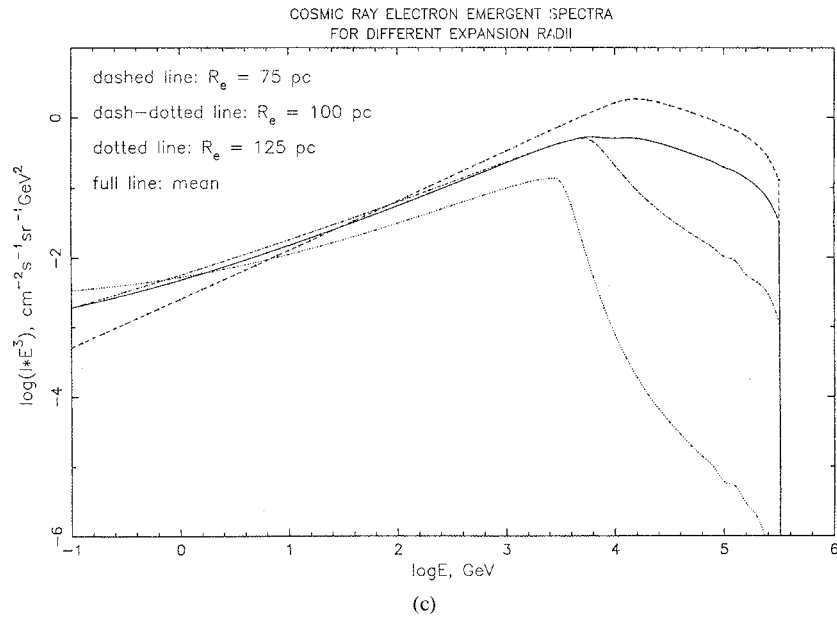


Figure 3. (Continued)

influence the value of R_e : the likelihood of a collision with another SNR, the fall of the cosmic ray energy density within the remnant to the ambient level and so on. The sensitivity of the emergent spectrum to the value of R_e in the electron case arises because of energy losses during the time in which the electrons have been trapped before emerging. We have examined the sensitivity of the results to R_e by re-working for $R_e = 75$ and 125 pc, values that we consider to encompass the likely range, and figure 3(c) gives emergent spectra for these three R_e -values; also included is a weighted mean over the range (1:2:1).

Turning to the likely spread of the energy loss factor, c , inspection of field maps of SNR coupled with images of remnants at various wavelengths suggests that the standard deviation of c is about $\pm 50\%$. Figure 3(d) shows the corresponding emergent spectra and the mean. Since the difference of the mean from our standard value (section 2.2) is small, we used the latter in later calculations.

2.3.2. *The adopted parameters.* To summarize the parameters, we have chosen the following:

- (i) the form $\eta = \exp(-(M/2)^2)$ for the acceleration efficiency for electrons;
- (ii) the SNR radius at which particles emerge is $R_e = 100 \pm 25$ pc;
- (iii) the spread in energy losses due to the non-uniformity of the ISM is taken to correspond to $\pm 50\%$ in the adopted mean c -value.

2.3.3. *The study of Donea and Biermann (2001).* These authors have very recently published a paper involving shock acceleration in SNR which gives an electron spectrum in the relativistic regime which has an exponent, 2.42 ± 0.04 , close to our value of ~ 2.49 . Their model involves ‘diffusive shock acceleration’, i.e. diffusion inside the shock layer, which takes energetic particles out of the shocked region, thereby steepening the spectrum. In a sense the model is similar to ours in that high energy particles are discriminated against, but of course the physics is quite different.

2.4. *The predicted electron spectra after propagation*

2.4.1. *Contribution from the galactic disk.* We proceed in the Monte Carlo analysis by taking the usual random distribution of SN in the ‘local’ part of the galaxy (5×10^4 SN in 10^8 yr over a radius 3.16 kpc centred on the Sun) and letting the electrons diffuse to the Earth when the Sun is outside the remnant. EW (2001a) gives the details; briefly, we adopt a mean lifetime for escape,

$$\tau(E) = 4 \times 10^7 E^{-0.5} \text{yr} \quad (7)$$

where E is in GeV and a diffusion coefficient appropriate to $H_G = 1$ kpc.

Figure 4(a) gives 50 spectra for the case of $M_0 = 2$, this being the value which gives good agreement with the observed spectral shape to $\log E = 2.5$ and, at the same time, the correct e/p ratio.

Considering $\log E > 2.5$, quite violent fluctuations in intensity are seen, caused by the presence or absence of a local SNR. This region is, in our view, analogous to the energy region near $\log E = 6$ (the ‘knee’) for protons.

Figure 4(b) shows the median spectrum of electrons with and without the efficiency factor; the reduction in intensity and increase in exponent, when η is included, are apparent. Also shown is the situation for protons, where we prefer a small, but finite correction for $\eta(M)$. It is important to note that the ensuing predicted e/p ratio is very close to that observed, i.e. fitting the slope causes e/p to fit as well.

Though the e/p ratio and its energy dependence, i.e. the shapes of the proton and electron spectra are correct, the absolute intensities are about eight to nine times lower than the experimental intensities. We regard this discrepancy as not very alarming, since the contribution from the galactic halo particles (see section 2.4.2), use of a higher local SN rate and a higher fraction of the explosion energy transferred into cosmic rays will bring about agreement of our calculated and observed absolute intensities. The halo factor is about a factor 2 (see the next section) and in the Berezhko *et al* (1996) study the energy fraction transferred to cosmic rays can easily reach 0.3 instead of our 0.1. The SN rate should be increased by at least 2 and adoption of these factors gives the necessary increase.

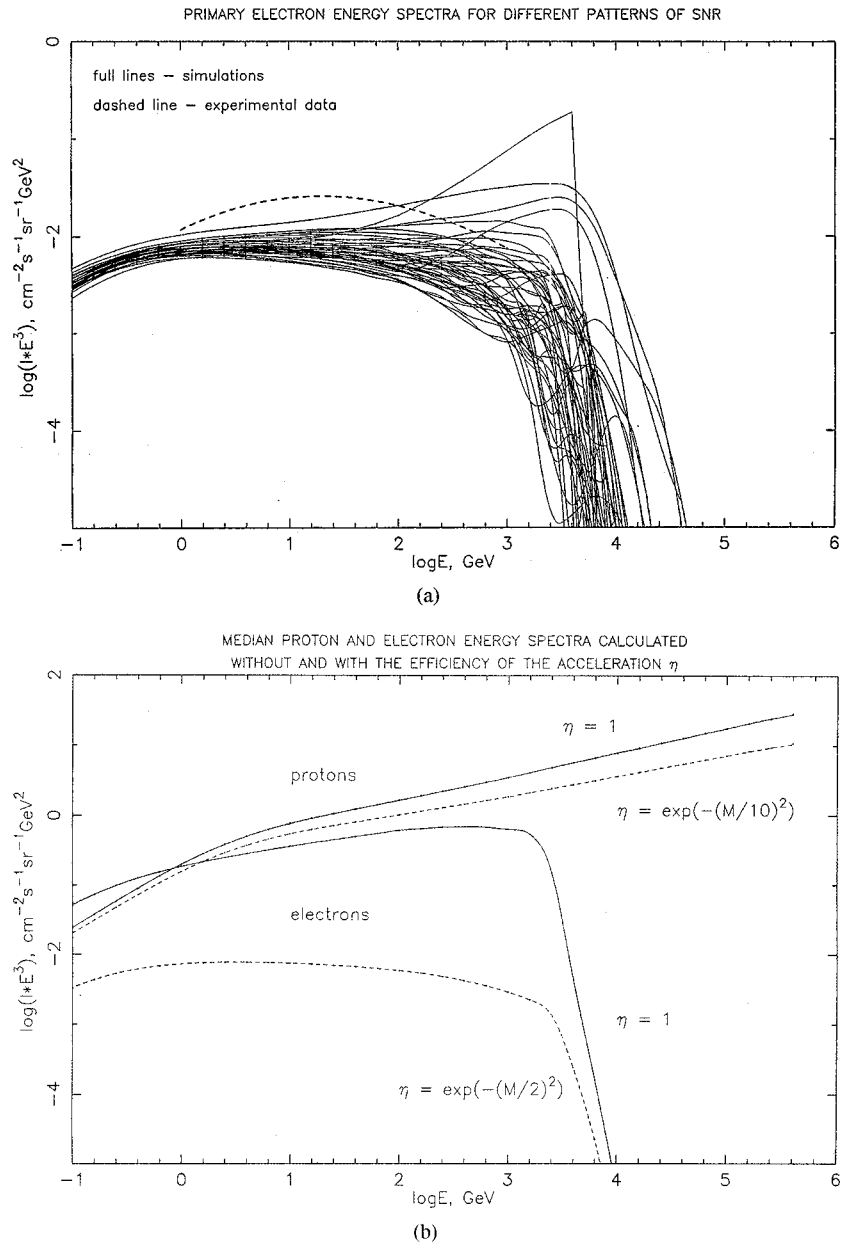


Figure 4. (a) Examples of predicted electron spectra for the preferred model. (b) Median spectra for both electrons and protons.

Figure 4(b) shows that the correct shape of the proton and electron spectrum and their e/p ratio can be obtained for the median spectra in the energy region not influenced by local sources using the acceleration mechanism which originally gave the flat slope of the emergent spectra with $\gamma = 2.15$ (but now gives $\gamma = 2.49$) without the assumption that the origin of the steep electron spectrum is an extreme fluctuation (Pohl and Esposito 1998).

2.4.2. Contribution from the galactic halo. In this section we consider the re-entrant particles from the halo.

As remarked in section 2.1 a reasonable choice of halo parameters is $H_H = 10$ kpc, $\tau_H = 10 \times \tau_{\text{disk}}$. In the region of energy where losses (other than escape) are unimportant, the halo component will have the same intensity as that of the disk component. This result follows from the fact that, approximately, within a cylindrical leaky box model, the ambient energy density is given by

$$\varepsilon_H = \varepsilon_D \frac{V_D \tau_H}{V_H \tau_D} = \varepsilon_D \frac{10}{10} = \varepsilon_D \quad (8)$$

where V and τ are the volume and the lifetime and subscripts H and D relate to the halo and the disk, respectively. In fact, the extra losses in the halo will cause a slightly earlier cut-off in energy and the factor of increase in the region of $\log E = 3$ will be somewhat less than 2. In view of the large fluctuations in intensity in this energy region it is not necessary to consider the reduction and an increase in intensity by a factor of two everywhere is sufficiently accurate.

For protons the increase is, indeed, a factor of two everywhere.

2.5. The spectral exponents

Figure 5 shows the frequency distribution of the spectral exponents for various energy ranges, in comparison with observation. Quite understandably, the spread at high energies is greater than the equivalent for the proton component, the reason being that the electrons are derived from sources which are nearer, where the fluctuations in number are greater. It will be noted that, apart from the difficult region below 1 GeV, there is agreement at all energies and not just at 10–100 GeV, where the fit to the experimental data was made.

3. The contribution from local sources

3.1. General remarks

Notwithstanding a certain scepticism towards our single source model, there is general agreement that for electrons local sources must, in principle, affect at least the highest energy intensities. The study of Kobayashi *et al* (1999) is a case in point; these researchers consider contributions from individual ‘sources’, e.g. Geminga, Vela, Loop I, and with their own model derive significant intensities above 500 GeV. This aspect, of contribution from ‘known’ sources, is considered, here, in the appendix. In what follows, we examine the likelihood of contributions from statistical fluctuations of local SN numbers and ages for our model.

3.2. Contributions from a ‘single source’

Figure 6 shows the probability distributions for particular contributions from a single source at the energy of 3 TeV. The distribution shows much higher sensitivity of electrons to the presence of a single local source, compared with protons, since their contribution to the electron intensity is much higher.

It is of interest to study the extent to which the signal that we have frequently claimed to exist for a single source would be apparent in the electron component. Figure 7 shows such a situation; namely, the same configuration of SN and ages gives a single source (SS) peak in both protons and electrons. The SS electron peak is seen to be remarkably sharp—its shape is consistent with expectation for this particular source (age $\sim 9.5 \times 10^4$ yr, distance 390 pc). It is unfortunate that the experimental data achieved so far cease at just the energy where such a

ELECTRON SPECTRUM SLOPE DISTRIBUTION

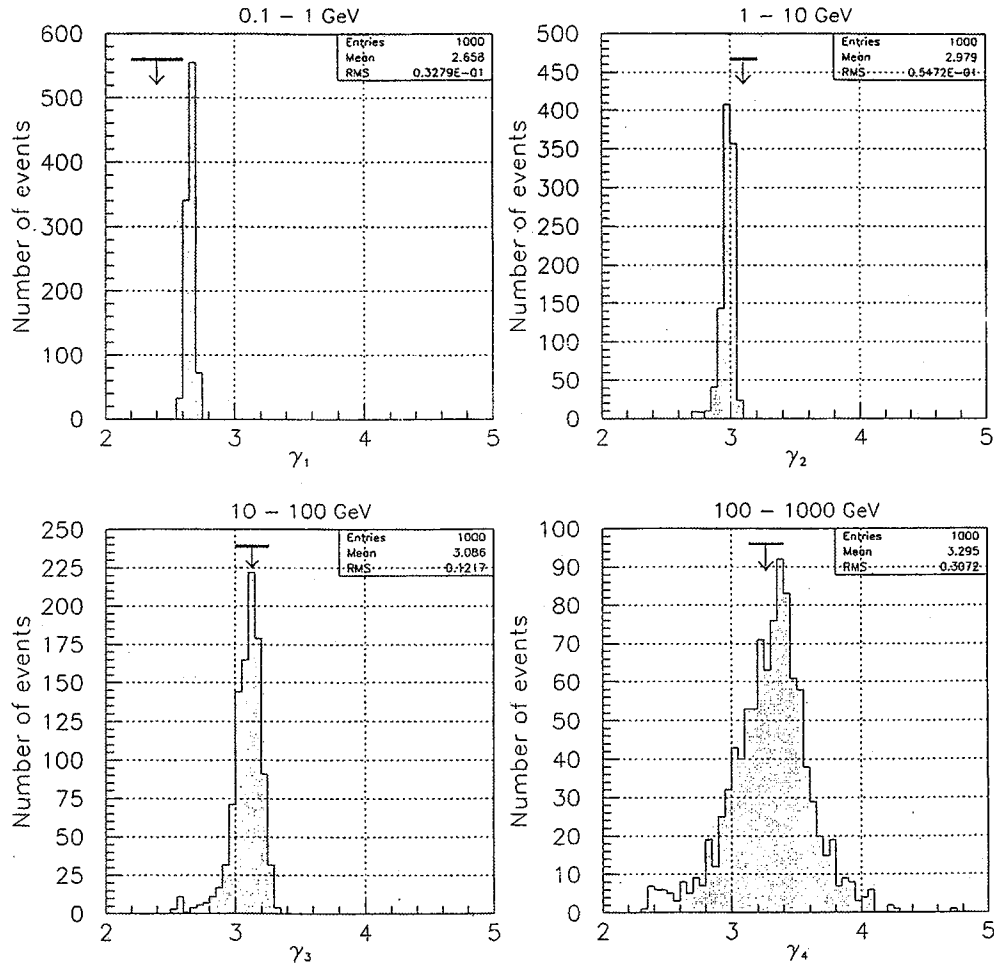


Figure 5. Frequency distribution of predicted exponents for the energy ranges indicated. The measured exponents (averaged over all the experiments) are indicated as small downward arrows above the distributions; their associated uncertainties are shown. Below 1 GeV the measured values (bars) come from studies of radio synchrotron radiation by Strong and Wolfendale (1978) and Webber *et al* (1992). The other bars represent the averages from the world survey data of Kobayashi *et al* (1999).

peak might be visible; specifically, approximately three electrons have been recorded so far at $\log E > 3$.

4. Fine structure in the general electron spectrum

An interesting feature of the measurements of the electron spectrum is the possible presence of ‘bumps’ at energies before the maximum energies, e.g. in the ‘BETS’ spectrum (Torii *et al* 1999) and the AMS spectrum (Alcaraz *et al* 2000). Similar evidence exists for positrons—see Coutu *et al* (1999). Figure 4(a), here, shows a somewhat similar behaviour, a not unexpected result because of the stochastic nature of the sources and the strong effect of energy losses for

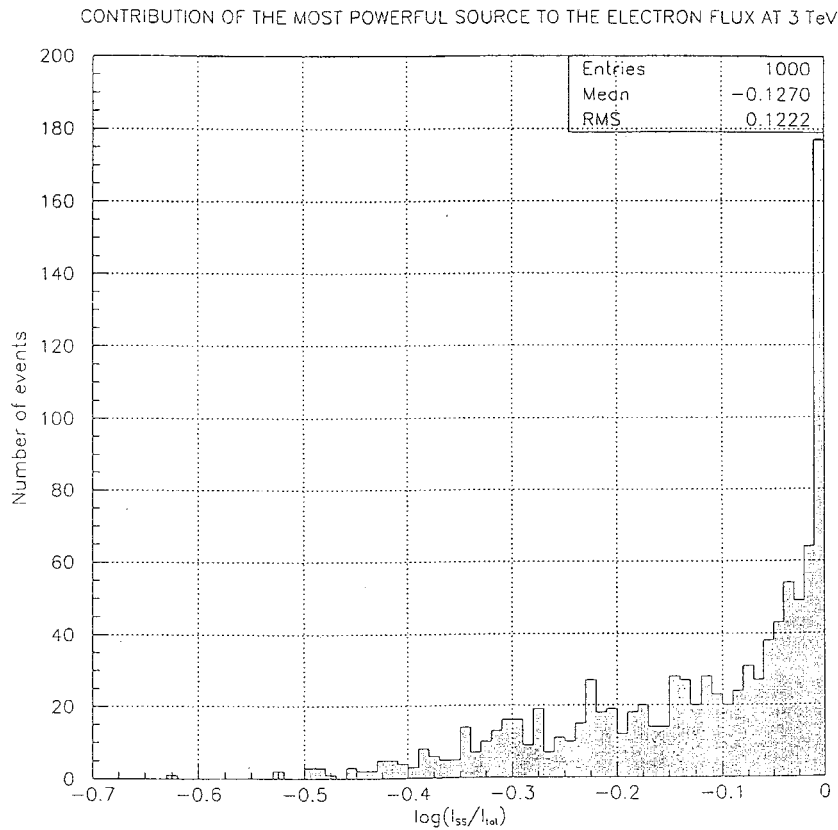


Figure 6. The fraction of the intensity at 3 TeV coming from a single most powerful source. It will be noted that the most likely contribution is 100% and the mean value is $10^{-0.127}$, i.e. 75%.

electrons; interestingly, even at energies in the region of $\log E = 2$, it is not uncommon for a single source to contribute some tens of per cent of the total intensity.

An attempt has been made to quantify the bumps by use of a similar technique to that used in Erlykin *et al* (1998) and later papers: ‘deviations from the running mean’ (actually, here, it is simply the difference between the intensity at $\log E = n$ and the mean of the intensity at $n + 0.2$ and $n - 0.2$). Figure 8 shows such ‘ Δ -values’ taken with a spacing of $\log E = 0.2$. It will be noted that with the exception of the lowest energy band ($\log E: 0-0.5$; $\langle E \rangle = 1.6$ GeV) the mean values are not inconsistent with zero. The behaviour in the first energy band is understandable in view of the systematic concavity of the energy spectrum here (see figure 3(a)). For the other regions, peaks and troughs appear with increasing amplitude and extrapolating a little above the maximum energy studied (1000 GeV) shows that $\Delta_{\text{RMS}} = 0.1$ at 2000 GeV.

Returning to the experimental data, most sets of data have rather large errors which would mask intensity variations less than about $\Delta \sim 0.1$. However, a few have what might be thought to be ‘interesting’ values and these are shown in the figure. None is significantly different from zero but it is important to get such possible variations in perspective.

The value of the plots is not so much in searching for the very small values of Δ expected on our model (at least below 100 GeV) but as providing a ‘background’ in searches for possible

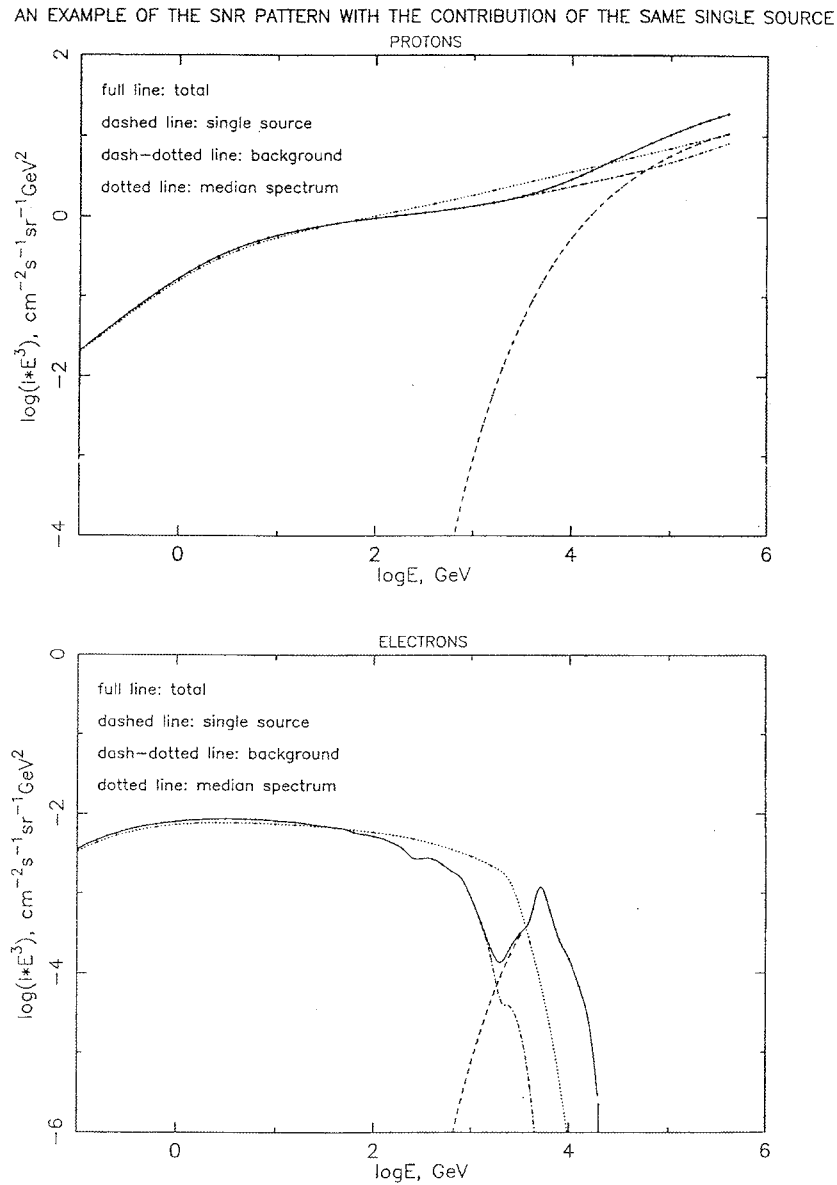


Figure 7. An example showing spectra for the situation where a ‘single source’ gives a big contribution to the proton spectrum. For electrons with an identical SN configuration, a strong SS peak appears.

evidence of exotic processes, i.e. electrons from the decay of hypothetical supersymmetric particles.

5. Other aspects of the electron results

5.1. Radio spectra from specific SNR

Ideally, it should be possible to check the form of the electron spectrum in individual SNR against results from figure 3(c). The relationship between the exponent of the electron

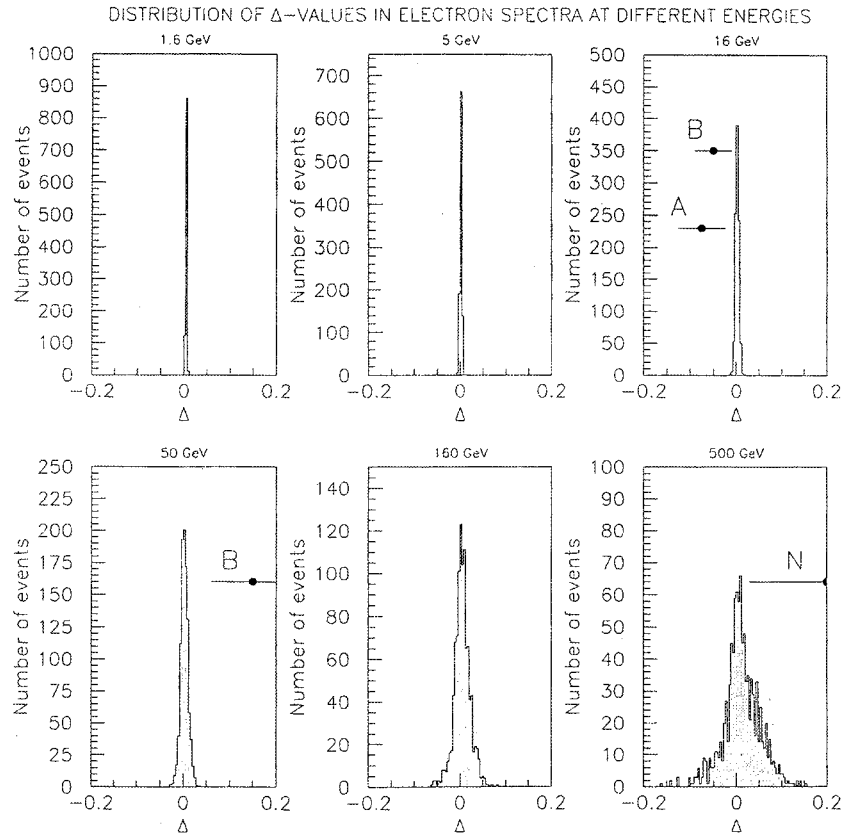


Figure 8. The frequency distribution of the Δ -values (the parameter which defines the irregularity of the spectrum). Most experimentally measured spectra show no ‘interesting’ dispersions outside the quoted errors, but these are always bigger than our expected dispersions. Actual values are just shown for three experiments: *B* (‘BETS 97–98’, Torii *et al* 1999), *N* (Nishimura *et al* 1995) and *A* (Alcaraz *et al* 2000). The predicted rms Δ -values are, for $\langle E \rangle = 1.6, 5, 16, 50, 160$ and 500 GeV (in units of 10^{-2}): 0.14, 0.24, 0.41, 0.82, 1.77 and 4.03.

spectrum, γ , and that of the power spectrum of radio, ν , is well known, $\gamma = 2\nu + 1$, so that a prediction can be made of ν versus SNR age or radius. In fact, the situation is one of great difficulty for a number of reasons:

- (i) spectral measurements are not available for many SNR,
- (ii) the spread from one SNR to another is considerable,
- (iii) energetic electrons from the associated pulsar are a worry (the CRAB nebula is a case in point, where ν is singularly small, 0.3, and the pulsar alone appears to be the ‘driving force’).

We have examined the available data on SNR (Green 1996) and determined the overall spread of the quoted slopes. The spread in ν extends from 0 to 1.0, namely, ν in $F(\nu_R) \propto \nu_R^{-\nu}$, ν_R being the radio frequency. The most probable value is $\nu = 0.5$ and the full width at half height is 0.35. For an SNR of radius 100 pc we expect $\gamma_e = 2.49$ and thus $\nu_R = 0.75$ but for a radius 50 pc, which encompasses most detected SNR, $\gamma \simeq 2.17$ and thus $\nu \simeq 0.58$. Such a value is well within the range observed.

Restricting attention to those SNR in the catalogue which have known distances, the median value of ν is 0.58. The median radius here is about 10 pc, for which we expect $\nu \sim 0.5$; again, there is no disagreement. Ideally it should be possible to see ν increasing with radius and there is an indication of this in the summary by Ginzburg and Syrovatsky (1965); however, the later study by Green (1996) does not confirm the trend. The problem seems to be the presence of a number of very low values of ν (≤ 0.3); these are probably due to electrons from associated pulsars, as distinct from SNR, as is the well-known case for the CRAB, already referred to.

5.2. The positron flux

Inspection of the data on the positron/electron ratio (see, e.g., the summary by Boezio *et al* 1999) shows evidence for an excess over conventional expectation at energies above 5 GeV (5–40 GeV). One possible explanation follows from our model, which relies on particles from previous SN ejecta as seed particles.

Attention is drawn to the role of ^{56}Ni and ^{56}Co , produced in the SN explosion, which, by its decay gives rise to the observed light curve. ^{56}Co decays with a lifetime of 77 d by the emission of a positron of maximum energy 1.5 MeV. Such an energy has a gyroradius greater than that for a thermal proton and will thus have a comparatively high injection efficiency. Thus, provided that a sufficient fraction of the 1.5 MeV positrons survive the initial high density SNR, a likely contender for the positron excess appears.

5.3. Extragalactic electrons

We return to the comment in the introduction about the importance of electrons for astronomy in general. A crucial point concerns the electron-to-proton ratio, which is found to be $\sim 1\%$ locally (at 10 GeV), and this value is usually assumed to be a ‘universal constant’. In fact, our model shows that the value of e/p will depend on the properties of the region in which the particles are accelerated, whatever the cause of the steepened electron spectrum ($\eta = f(M)$ or . . .). There may well be regions where e/p is much nearer unity and the effect on the overall universal energy content in relativistic particles could well be profound, insofar as $e/p = 1\%$ is often assumed in the calculation of the energy of a system.

Another aspect, needing further study, is the well-known difficulty in some objects, e.g. the CRAB nebula and M87 (see Robson 1996), of explaining the presence of energetic electrons far from the usual ‘central engine’—pulsar and black hole, respectively. Some form of shock acceleration can be involved. In our model such shocks, although weak, could be very efficient because of the presence of low energy—but still relativistic—electrons ‘left over’ from the initial process; the injection efficiency for these particles could be very high. A very recent paper by Leahy *et al* (2001) on the radio lobes of jets may also have relevance. For a number of lobes (3C, 28, 295, 310, 388, Her A and Cyg A) a comparison of radio and x-ray observations leads to the conclusion that relativistic protons may account for less than ten times the electron component (rather than the usual 100 times). It is true to say, however, that there are complications involved due to the presence of relativistic shocks at the ends of the lobes.

6. Conclusions

We have put forward a model for cosmic ray acceleration which differs from that usually adopted in that it attributes the low e/p ratio and somewhat steeper energy spectrum than that

for protons—in the region where electron energy losses are negligible—to differences in the injection efficiency formalism.

A detailed Monte Carlo analysis gives the frequency distribution of spectral slopes and the magnitude of spectral ‘curvature’ (the Δ -excess), both as a function of energy. The latter should prove useful in searches for ‘bumps’ attributable to particles from the decay of hypothetical supersymmetric particles.

Concerning our single source model, it is demonstrated that the electron energies so far accessible are not quite high enough to enable conclusions to be drawn. Nevertheless, the energies achieved *are* such that local sources probably do make a significant contribution.

Concerning the validity of the SNR model for explaining the bulk of the cosmic radiation—to 10^{16} eV, at least, in its simple form—it has been demonstrated that there are no problems with the electron component. The oft-quoted shortage of TeV gamma rays for an SNR origin of the relevant cosmic ray ‘primaries’ is probably illusory—see, for example, Berezhko and Volk (1999). The problem is a straightforward one, that SNR have high efficiency for high energy particles in the low density hot ISM (see, e.g., Erlykin *et al* 1998) and here the target for high energy gamma ray production is too ‘thin’.

Turning to the need for an electron emergent spectrum steeper than the canonical E^{-2} spectrum, although in principle it can be argued that fluctuations in the expected spectral slope can give the measured spectrum, these would need to be excessive, as can be seen by reference to figure 5, where it is shown that, for E_e : 10–100 GeV, the hwhm is $\Delta\gamma = 0.10$. Thus, if we were to adopt an emergent spectrum with E^{-2} , the measured spectrum would have $\gamma = 2.5$ (the extra 0.5 coming from the galactic lifetime exponent), i.e. $\Delta\gamma = 0.6$ away from observation.

Acknowledgments

The authors are grateful to The Royal Society and the Particle Physics and Astronomy Research Council for financial support. We wish to thank the following for helpful comments: W I Axford, E G Berezhko, D R Flower, J G Kirk, J P Leahy and the unknown referees.

Appendix. Electron energy from known sources

Torii *et al* (1999) and Kobayashi *et al* (1999) have given the results of calculations of the spectra expected at Earth from a number of ‘known’ sources. The analyses did not involve SNR expansion in the manner described here, but sources of electrons (presumably pulsars) which gave rise to particular energy outputs. Specifically, outputs of 10^{48} erg were assumed and particular forms for the diffusion coefficient versus energy were adopted. The results of Kobayashi *et al* showed particularly dramatic fluxes.

We have used our model to make predictions and these are shown in figure A1. The ages and distances are indicated. Unlike in the predictions of Kobayashi *et al* we do not expect a flux of electrons from Vela—the particles have not yet arrived. Also indicated is the region occupied by the experimental data (from the summary by Kobayashi *et al*). Although the ‘predictions’ are a decade below the observations, when it is borne in mind that the injection energy may be as much as a factor of three above that assumed (see section 2.4) it is clear that one or more of these sources is on the verge of detection.

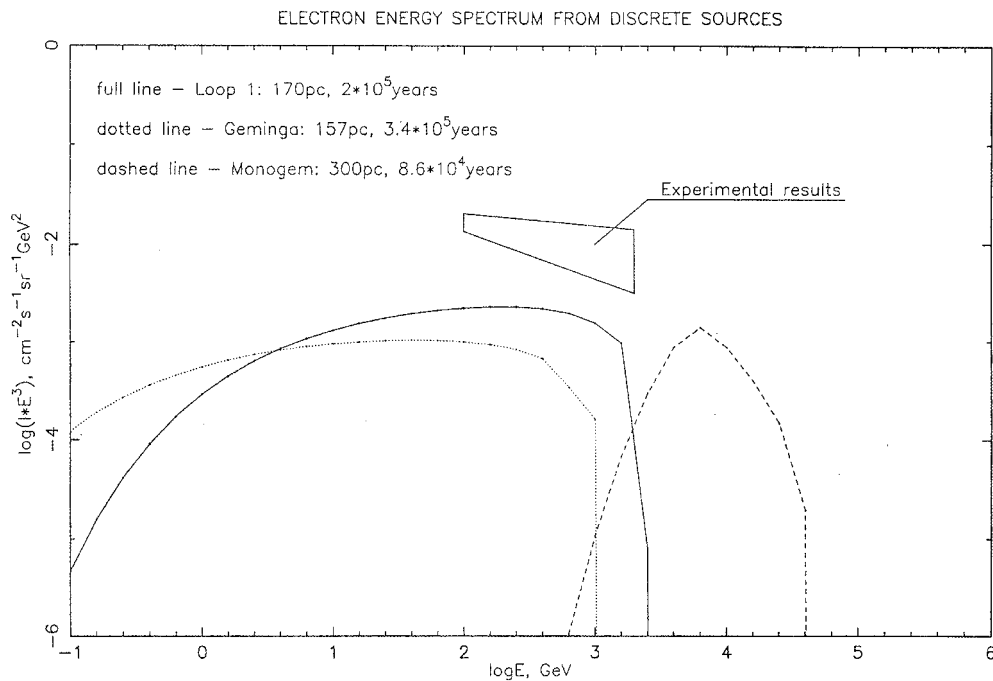


Figure A1. Predicted spectra for the SNR listed, in comparison with the experimental results (from the summary by Kobayashi *et al* (1999)). The electron energy input could be higher by a factor ~ 3 and thus the sources could contribute to the total to a significant degree.

References

- Aharonian F A, Atoyan A M and Völk H J 1995 *Astron. Astrophys.* **294** L41
Alcaraz J *et al* 2000 *Phys. Lett. B* **484** 10
Atoyan A M, Aharonian F A and Völk H J 1995 *Phys. Rev. D* **52** 3265
Axford W I 1981 *Proc. 17th Int. Cosmic Ray Conf. (Paris)* vol 12 p 155
Barbiellini G *et al* 1997 *Proc. 25th Int. Cosmic Ray Conf.* vol 3 p 221
Barwick S W *et al* 1998 *Astrophys. J.* **498** 779
Berezhko E G, Elshin V K and Ksenofontov L T 1996 *Sov. Phys.-JETP* **82** 1
Berezhko E G and Völk H J 1999 *Proc. 26th Int. Cosmic Ray Conf. (Salt Lake City)* vol 4 p 377
Blandford R D and Ostriker J P 1980 *Astrophys. J.* **237** 793
Boezio M *et al* 1999 *Proc. 26th Int. Cosmic Ray Conf. (Salt Lake City)* vol 3 p 57
Boezio M *et al* 2000 *Astrophys. J.* **532** 653
Chi X and Wolfendale A W 1991 *The Interstellar Dish-Halo Connection in Galaxies* ed H Bloemen (Dordrecht: Kluwer Academic Publishers)
Coutu S *et al* 1997 *Proc. 25th Int. Cosmic Ray Conf. (Durban)* vol 4 p 213
Coutu S *et al* 1999 *Astropart. Phys.* **11** 429
Denskat K U *et al* 1983 *J. Geophys.* **54** 60
Donea A-C and Biermann P L 2001 *Proc. 27th Int. Cosmic Ray Conf. (Hamburg)* vol 5 p 1795
Ellison D C, Berezhko E G and Baring M G 2000 *Astrophys. J.* **540** 292
Ellison D C, Drury L O'C and Meyer J-P 1997 *Astrophys. J.* **487** 197
Ellison D C and Reynolds S P 1991 *Astrophys. J.* **382** 242
Erlykin A D and Wolfendale A W 2001a *J. Phys. G. Nucl. Part. Phys.* **27** 941
Erlykin A D and Wolfendale A W 2001b *J. Phys. G. Nucl. Part. Phys.* **27** 959
Erlykin A D and Wolfendale A W 2001c *J. Phys. G. Nucl. Part. Phys.* **27** 1709
Erlykin A D, Wolfendale A W and Vahia M N 1998 *Frontier Objects in Astrophys. and Part. Phys. (Vulcano Workshop)* ed F Giovannelli and G Mannocchi p 455

- Erlykin A D *et al* 1996 *Astron. Astrophys.* **120** 397
- Flower D R 2001 Private communication
- French D K 1977 *PhD Thesis* University of Durham
- Ginzburg V L and Syrovatsky S J 1964 *The Origin of Cosmic Rays* (Oxford: Pergamon)
- Golden R L *et al* 1984 *Astrophys. J.* **287** 622
- Golden R L *et al* 1994 *Astrophys. J.* **436** 769
- Green D A 1996 *Catalogue of SNR* University of Cambridge
- Grenier I A and Perrot C 1999 *Proc. 26th Int. Cosmic Ray Conf. (Salt Lake City)* vol 3 p 476
- Haslam C G T, Salter C J and Stoffel H 1981 *Origin of Cosmic Rays (IAU Symp. 94)* ed G Setti, G Spada and A W Wolfendale p 217
- Higdon J C, Lingenfelter R E and Ramaty R 1999 *Proc. 26th Int. Cosmic Ray Conf. (Utah)* vol 4 p 144
- Kaplan S A and Tsyтович V N 1973 *Plasma Astrophysics* (Oxford: Pergamon)
- Kobayashi T *et al* 1999 *Proc. 26th Int. Cosmic Ray Conf. (Salt Lake City)* vol 3 p 61
- Leahy J P, Gizani N and Tsakiris D 2002 *Particles and Fields in Radio Galaxies (APS Conf. Series)* ed R A Laing and K M Blundell at press
- Levinson A 1992 *Astrophys. J.* **401** 73
- Melrose D B 1968 *Astrophys. Space Sci.* **2** 171
- Moskalenko I V and Strong A W 1998 *Astrophys. J.* **493** 694
- Nishimura J *et al* 1995 *Proc. 24th Int. Cosmic Ray Conf. (Rome)* vol 3 p 29
- Pineau des Forêts G *et al* 1987 *Mon. Not. R. Astron. Soc.* **227** 993
- Pohl M and Esposito J A 1998 *Astrophys. J.* **507** 327
- Robson I 1996 *Active Galactic Nuclei* (Chichester: Wiley)
- Schmitz H *et al* 2001 *Proc. 27th Int. Cosmic Ray Conf. (Hamburg)* vol 6 p 2022
- Shen C S 1970 *Astrophys. J.* **162** L181
- Shen C S and Mao C Y 1971 *Astrophys. Lett.* **9** 169
- Shimada N and Hoshino M 2000 *Astrophys. J.* **543** L67
- Stephens S A 1990 *Proc. 21st Int. Cosmic Ray Conf. (Adelaide)* vol 11 p 99
- Stephens S A 1999 *Proc. 26th Int. Cosmic Ray Conf. (Salt Lake City)* vol 4 p 241
- Strong A W and Wolfendale A W 1978 *J. Phys. G: Nucl. Part. Phys.* **4** 1793
- Syrovatskii S I 1959 *Sov. Astron. AJ* **3** 22
- Tang K-K 1984 *Astrophys. J.* **278** 881
- Torii S *et al* 1999 *Proc. 26th Int. Cosmic Ray Conf. (Salt Lake City)* vol 3 p 53
- Webber W R *et al* 1992 *Astrophys. J.* **390** 96